Ultrasound in Med. & Biol., Vol. 48, No. 12, pp. 2449–2460, 2022

0301-5629/$ - see front matter

https://doi.org/10.1016/j.ultrasmedbio.2022.07.001

● *Original Contribution*

ULTRASOUND-STIMULATED MICROBUBBLES ENHANCE RADIATION-INDUCED CELL KILLING

Giulia McCorkell,* Masao Nakayama,† Bryce Feltis,‡ Terrence Piva,‡ and Moshi Geso*

* Department of Medical Radiations, School of Health and Biomedical Sciences, RMIT University, Victoria, Australia; † Division of Radiation Oncology, Kobe University Graduate School of Medicine, Hyogo, Japan; and ‡ Department of Human Bioscience, School of Health and Biomedical Sciences, RMIT University, Victoria, Australia

(*Received* 2 *August* 2021; *revised* 29 *March* 2022; *in final form* 1 *July* 2022)

Abstract—Recent *in vivo* studies using ultrasound-stimulated microbubbles as a localized radiosensitizer have had impressive results. While *in vitro* studies have also obtained similar results using human umbilical vein endothelial cells (HUVEC), studies using other cell lines have had varying results. This study was aimed at investigating any increases in radiation-induced cell killing *in vitro* using two carcinoma lines not previously investigated before (metastatic follicular thyroid carcinoma cells [FTC-238] and non-small cell lung carcinoma cells [NCI-H727]), in addition to HUVEC. Cells were treated using a combination of 1.6% (v/v) microbubbles, ~90 s of 2-MHz ultrasound (mechanical index = 0.8) and 0–6 Gy of kilovolt or MV X-rays. Cell viability assays obtained 72 h post-treatment were normalized to untreated controls, and analysis of variance was used to determine statistical significance. All cells treated with combined ultrasound-stimulated microbubbles and radiation exhibited decreased normalized survival, with statistically significant effects observed for the NCI-H727 cells. No statistically significant differences in effects were observed using kV compared with MV radiation. Further studies using increased microbubble concentrations may be required to achieve statistically significant results for the FTC-238 and HUVEC lines. (E-mail: moshi.geso@rmit.edu.au) **© 2022 The Author(s). Published by Elsevier Inc. on behalf of World Federation for Ultrasound in Medicine & Biology. This is an open access article under the CC BY-NC-ND license (http://creativecommons.org/licenses/by-nc-nd/4.0/).**

Key Words: **Ultrasound, Microbubble, Radiation, Cell death, Radiosensitization.**

INTRODUCTION

Microbubbles (MB) have long been used as contrast agents to improve image quality in ultrasound (US) cardiac imaging (Kaul 2008). Their size is similar to that of the average erythrocyte, meaning they remain within the endovascular borders during their travel from the site of injection to the site of interest. This feature has resulted in MB also being investigated for a variety of focused therapeutic purposes, as they can be "burst" using higher US intensities once at the site of interest. This "bursting" creates localized biophysical disruptions in the cell's vicinity (Ebben et al. 2017; Zhu et al. 2019) and, if loaded with a treatment agent, can also deliver a localized therapeutic payload (Liu et al. 2006).

Address correspondence to: Moshi Geso, Department of Medical Radiations, Level 8, Building 201, RMIT University, PO Box 71, Bundoora 383, Victoria, Australia. E-mail: moshi.geso@rmit.edu.au

In vivo *studies*

As a result, there has been recent interest in using ultrasound-stimulated microbubbles (USMB) as localized radiosensitizers of radiation treatment (RT), with *in vivo* studies reporting some promising results. Czarnota et al. (2012) reported a statistically significant increase in mean animal survival from 19d with RT alone to 28 d using USMB and RT together (USMB + RT). PC3 human prostate cancer xenografts in mice were treated twice weekly with USMB in conjunction with 24 Gy in 12 fractions of 160-kVp X-rays delivered four times a week for 3 wk. Daecher et al. (2017) reported a mean animal survival of 11 d with RT alone compared with 35 d using USMB + RT in treating human hepatocellular carcinoma xenografts in nude rats. In this study the xenografts were treated with USMB, followed by a single dose of 5-Gy kilovolt X-rays delivered using 4- × 1.25-Gy beams. Two animals treated with USMB + RT exhibited complete tumor control, with tumor reduction or stability observed 50 d post-treatment. Eisenbrey et al.

(2018) observed a statistically significant growth delay for MDA-MB-231 human adenocarcinoma breast xenografts in mice administered USMB + RT compared with the controls administered US and oxygen MB alone ($p = 0.03$) or US and RT in the absence of MB ($p = 0.01$). Animals were treated with in-house manufactured oxygen or nitrogen USMB and a single fraction of 5 Gy using 310-kV X-rays.

Other *in vivo* studies have also determined that USMB + RT increase tumor cell death 24 h after treatment. Al-Mahrouki et al. (2014), using clonogenic assays from excised PC3 xenografts in mice, reported decreases in cell survival from 45.5% for 2 Gy alone to 26.8% for USMB + 2Gy, and from 38.2% for 8 Gy alone to 14.4% for USMB + 8 Gy, respectively. Lai et al. (2016), using *in situ* end labeling (ISEL) staining, reported increased rates of tumor death for MDA-MB-231 xenografts in Swiss nude mice of 3.4- and 2.3-fold respectively, for USMB + 2 Gy or USMB + 8 Gy treatments compared with 2- or 8-Gy RT alone.

It has been proposed that USMB + RT behaves as a biophysical vascular disruptor *in vivo*, acting primarily on endothelial cells to disturb tumoral blood supply (El Kaffas and Czarnota 2015). As a result of downstream vascular disruption, overall tumor control can be achieved at much lower radiation doses as microvascular collapse and rapid vascular shutdown lead to secondary tumor cell death once upstream cells become starved of nutrients and oxygen.

In vitro *studies*

Consequently, three *in vitro* studies were centered around human umbilical vein endothelial cells (HUVEC) using 3.3% (v/v) MB, 30 s of US with a mechanical index of 0.8 and between 0 and 8 Gy of 160-kVp X-rays. Clonogenic assays (normalized to control) revealed an increase in cell death from 67% for 8 Gy alone ($p < 0.014$) to 95% for USMB + 8 Gy ($p < 0.002$) (Al-Mahrouki et al. 2012), and a decrease in cell survival from 8% using 2 Gy alone to 1% using USMB + 2 Gy (Nofiele et al. 2013). The third study using HUVEC (Al-Mahrouki et al. 2015), found that treatment with USMB alone or USMB + RT caused cell membrane distortion, which was not evident in cells treated with RT alone, suggesting multiple mechanisms of cell damage may be achieved through the combined USMB + RT treatment.

Other *in vitro* studies investigating direct tumor cell radiosensitization using USMB have also been conducted. Karshafian et al. (2009) exposed acute myeloid leukemia (AML-5) cells to varying concentrations of MB, differing US pressures and 2−8 Gy of 160-kVp X-rays, and observed that cell viability decreased with increased MB concentration until maximal death was achieved at ~1.6% (v/v). Higher USMB levels did not increase cell killing but rather conferred a slightly protective effect. When AML-5 cells were exposed to 570-kPa US peak negative pressure (PNP) and 3.3% (v/v) USMB, cell viability was 71 ± 7% which was higher than that seen for cells exposed only to 4-Gy radiation (55 ± 5%). The order of treatment (*i.e.,* USMB followed by RT compared with RT followed by USMB) was found to have minimal impact on cell viability. Clonogenic assays were 11% for 2 Gy alone versus 2.5% for USMB + 2 Gy normalized to control (no treatment). Clonogenic survival also fell in another study (Karshafian et al. 2010), when PC3 and KHT-C murine fibrosarcoma cells were treated with USMB + 3 Gy (PC3 17% and KHT-C 34%, respectively) compared with RT alone (PC3 50% and KHT-C 75%, respectively). In this study, treatment order and time between treatments affected clonogenic survival, with greatest decreases in clonogenic viability seen when PC3 cells were exposed to USMB followed by immediate 3-Gy treatment (17%), compared with that of KHT-C cells treated with USMB followed by a 3-h gap before being exposed to 3 Gy (30%).

Deng et al. (2018) treated NCE-2 nasopharyngeal carcinoma cells with 3% (v/v) perfluropropane-based USMB, administered 24 h prior to exposure to 2- or 8-Gy RT. Cell viability was measured using the 3-(4, 5-dimethyl-2-thiazolyl)-2,5-diphenyl-2-*H*-tetrazolium bromide (MTT) assay 24, 48 and 72 hours post-treatment. Significant ($p < 0.01$) decreases in viability for NCE-2 cells treated with USMB + 2 Gy compared with 2 Gy were observed at 48 h, and at 72 h, USMB + RT significantly increased cell death for both radiation doses.

At a cellular level, USMB has previously been used to increase cell membrane permeability via the induction of sonoporation effects (Fan et al. 2014; Lentacker et al. 2014; Osei and Al-Asady 2020), and several early phase I clinical trials have subsequently confirmed the translational possibilities of this as a novel treatment modality (Dimcevski et al. 2016; Wang et al. 2018). It is thought that the combination of these sonoporation effects on cell membranes works synergistically with DNA damage arising from ionizing radiation to produce the enhanced tumor cell death seen through the combination of USMB and RT (Al-Mahrouki et al. 2012).

However, in a study of human pharyngeal squamous carcinoma (FaDU) cells, no differences between cells treated with USMB + RT and those treated with RT alone were observed in clonogenic assays (Lammertink et al. 2016). In this study the cells were exposed to 1 μg/mL cisplatin and USMB (700 μL of SonoVue) 24 h before being treated with varying doses of MV γ-rays (2, 4, 6, 8 or 10 Gy). The addition of USMB did not enhance any further damage than that elicited by RT alone in these cells.

As this study stands in stark contrast to all other research to date, the purpose of our study was to investigate the role of USMB in directly enhancing radiation-induced tumor cell killing *in vitro*. Two tumor cell lines not previously investigated before were used to determine whether direct USMB radiosensitization could be achieved for both a primary and metastatic cancer cell line. NCI-H727 cells are from a primary non-small cell lung carcinoma (NSCLC), while FTC-238 cells are from a metastatic follicular thyroid carcinoma deposit in lung tissue. Lung cancer is the most common cause of cancer death worldwide (World Health Organization), and radiotherapy treatment of lung lesions is challenging (Piperdi et al. 2021), hence the need to identify any means of radiotherapy dose enhancement available for these types of tumors. HUVEC were also investigated to allow for comparisons with existing published data (Al-Mahrouki et al. 2012, 2015). Definity MB were selected as they are the only commercially available MB approved for clinical use in Australia, and clinical hardware was used to provide US simulation. Both kilovolt (kV) and megavolt (MV) X-rays were used to investigate if different radiation energies enhance the cytotoxic effect of USMB, as previously it was reported that MV energies may not (Lammertink et al. 2016).

METHODS

Cell lines and culture conditions

Experiments were performed using HUVEC, FTC-238 (lung metastasis of follicular thyroid carcinoma) and NCI-H727 (non-small cell lung carcinoma). HUVEC (Catalog No. C2519A, pooled donor) were purchased from Lonza (Walkersville, MD, USA). FTC-238 and NCI-H727 cell lines were supplied by the European Collection of Cell Cultures (ECACC; Salisbury, UK) as Catalog Nos. 94060902 and 94060303, respectively, and were purchased from CellBank Australia (Westmead, Australia). All cell lines have been previously described (Takahashi et al. 1989; Goretzki et al. 1990; Dos Santos et al. 2018).

Cells were maintained according to the manufacturer's instructions and incubated at 37˚C, 5% CO_2 and 95% humidity. HUVEC were cultured using the EGM-2 Endothelial Cell Growth Medium-2 BulletKit from Lonza (Catalog No. CC-13162). FTC-238 cells were cultured using DMEM:F12 (Catalog No. D8437, Sigma-Aldrich, Sydney, Australia), supplemented with 5% fetal bovine serum (FBS, Corning, Catalog No. 35-076-CV supplied by Fisher Biotec, Wembley, Australia) and 1% penicillin−streptomycin (Pen-Strep, Catalog No. 15070063, Sigma-Aldrich). NCI-H727 cells were cultured in RPMI-1640 (Catalog No. 11875093, Thermo Fisher, Scorsby Australia), supplemented with 10% FBS and 1% Pen-Strep.

Plating and MTS assay optimization

Cell proliferation assays were initially optimized in the absence of treatments using CellTiter 96 Aqueous One Solution Cell Proliferation Assay (Catalog No. G3582, Promega, Australia). The MTS tetrazolium compound (3-(4,5-dimethylthiazol-2-yl)-5-(3-carboxymethoxyphenyl)-2-(4-sulfophenyl)-2*H*-tetrazolium) is similar to the MTT compound used in previous studies (Deng et al. 2018), and is bio-reduced by viable cells into a colored formazan product that can be analyzed via colorimetry. Cells are incubated with the reagent for between 1 and 4 h, and then absorbance readings were taken at 490 nm in a 96-well plate reader. The amount of formazan product measured by absorbance is directly proportional to the number of viable cells in the culture (Promega Corp. 2012).

Cell seeding densities and MTS development times were optimized to achieve 80% confluence at 72 h post-treatment for each cell line, as summarized in Table 1. This level of confluence was chosen to avoid any potential effects of contact-dependent cell signaling or contact inhibition, and 72 h is consistent with the manufacturer's instructions for cell proliferation studies and other experiments using this assay (Smith et al. 2006; Promega Corp. 2012; Youkhana et al. 2017) and the MTT assay (Deng et al. 2018). Because of the number of treatment conditions investigated in this study, the MTS assay was selected as it allows for high-volume throughput and is similar to the MTT assay that has demonstrated equivalence to the clonogenic assay (Buch et al. 2012).

HUVEC and FTC-238 cells from stock cultures were plated into T25 tissue culture flasks (Sigma-Aldrich, Catalog No. CLS430639). Because of supply issues, NCI-H727 cells were plated into T12.5 flasks (Bio-Strategy, Catalog No. BDAA353107, Tullamarine, Australia) which were as high as the T25 flasks (2.62 cm), but were 3.6 cm longer and 0.79 cm wider. Cells at the designated seeding densities were allowed to adhere overnight in their respective flasks for ∼14−16 h before treatment. Eight flasks were prepared for each

Table 1. Cell seeding densities and MTS development times

Cell line	Flask size (cm)	Seeding density (cells/flask)	MTS development time (min)
HUVEC	T25	8,000	25
FTC-238	T25	12,000	25
NCI-H727	T12.5	50,000	15

HUVEC = human umbilical vein endothelial cells; MTS = 3-(4,5-dimethylthiazol-2-yl)-5-(3-carboxymethoxyphenyl)-2-(4-sulfophenyl)-2*H*-tetrazolium.

experiment—three technical replicate control flasks (no treatment), one USMB-alone flask (USMB), and two flasks for each radiation dose level, one with USMB and one without (*i.e.,* 3 Gy, USMB + 3 Gy, 6 Gy and USMB + 6 Gy). Each experiment was performed in triplicate, with separate experiments run for kV and MV X-ray energies using the HUVEC and FTC-238 cell lines. Concurrent experiments were undertaken for NCI-H727 cells in which 12 flasks were prepared for each experiment: four for kV flasks and four for MV flasks in addition to four 0-Gy flasks (*i.e.,* three controls and one USMB). This experiment was also performed in triplicate.

Pre-treatment preparation

Two hours prior to treatment, cells grown in T25 flasks (volumes used for the T12.5 flasks were half that described here) were washed using 5 mL of phosphate-buffered saline (PBS, Thermo Fisher, Catalog No. 70011069), and detached from their adherent state using 2 mL of 0.25% trypsin−EDTA (Thermo Fisher, Catalog No. 25200056). Flasks of both sizes were then filled with 30 mL of cell-line specific complete medium and were periodically gently shaken throughout treatments to ensure cells did not re-attach. Definity Microbubbles (Lantheus Medical Imaging, Inc, supplied by Global Medical Solutions, Keilor Park, Australia) were activated using the Vialmix activation device (Lantheus Medical Imaging, Inc) according to the manufacturer's instructions (Lantheus Medical Imaging, Inc), and 480 μL was added to the relevant treatment flasks to give a final microbubble concentration of 1.6% (v/v) (~2.8 × 109 MB/flask), which was close to that described in other *in vitro* studies (Karshafian et al. 2009, 2010; Al-Mahrouki et al. 2012, 2015; Nofiele et al. 2013; Deng et al. 2018).

The culture flasks including the untreated controls were then transported offsite to the treatment facility at either the Australian Radiation Protection and Nuclear Safety Agency (ARPANSA) (Yallambie, Australia) or the GenesisCare Epping Radiation Oncology Centre (EPROC) (Epping, Australia). Travel time to and from these facilities was around 20 min each way, with the cells out of the 37°C incubator for ~90 min.

Ultrasound treatment

Once onsite at the treatment facility, ultrasound sonication was applied using the LOGIQi Portable Ultrasound with the 4C-RS transducer in simple 2-D B-mode (GE Healthcare, Paramatta, Australia). Here, 2-MHz frequency ultrasound was applied directly to the flask using a coupling gel, with a focal point of 3.25 cm and depth of 4 cm, resulting in a frame rate of 61 Hz. Two megahertz was selected to provide a wide beam that exposed the greatest surface area and minimized attenuation from the polystyrene walls of the flask. The depth of 4 cm was selected to ensure the entire height of the flask was exposed within the near zone. The transducer was moved across the flask for ~90 s until the opaque, milky-white microbubbles had burst and the medium had returned to its normal transparency. Previous preliminary studies using colorimetry and microscopy had revealed that this visual change correlated with the bursting of the microbubbles and this visual change, along with the ultrasound setup, can be seen in Figure 1. The flasks were then immediately exposed to either 0, 3 or 6 Gy of kV or MV X-rays. The three control flasks were left untreated, and the USMB-only flask received ultrasound sonication in the absence of ionizing radiation.

Radiation treatment

Six-megavolt X-rays were delivered using either a Varian iX (EPROC) or an Elekta Synergy Linear Accelerator (ARPANSA), with the same linear accelerator used for each repeat of an individual experiment. Flasks were laid flat on the treatment couch on top of 10 cm of solid water, with a source-to-surface distance (SSD) of 100 cm set to the top of the solid water from a gantry angle of 0°. Next, 2 cm of solid water was then placed on top of the flasks to provide a buildup region, and both RT ± USMB flasks were irradiated simultaneously using a 20- × 20-cm field size to cover both flasks. Figure 2 is a schematic of this setup.

The 100-kVp X-rays (average energy: 42.5 kV) were delivered using a Model X80 X-Ray Beam irradiator by Hopewell Designs (ARPANSA). A 100-cm SSD was set to the baseplate of the unit before the RT ± USMB flasks were taped vertically to the baseplate (see Fig. 3). A 10-cm circle field size was used to expose both flasks concurrently. As the dose rate from this unit was 6 mGy/s, the 3- and 6-Gy doses took 491.8 and 983.6 s to deliver, respectively, which was the determining factor in the selection of X-ray doses used in this

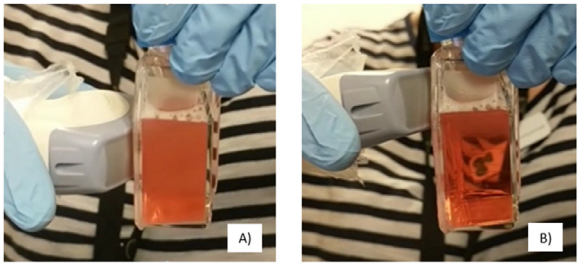

Fig. 1. Images of the ultrasound exposure revealing how the transducer was moved across the surface of the flask for ~90 s until the milky white microbubbles as seen in (A) had burst and the medium returned to its normal transparency (B).

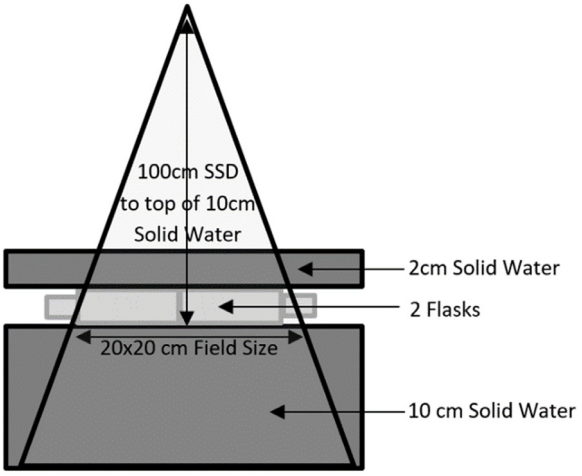

Fig. 2. Schematic illustrating the experimental setup for megavolt X-ray exposures. Radiation therapy ± ultrasound-stimulated microbubble flasks were placed on top of 10 cm of solid water, with a 100-cm source-to-surface distance set to the top of the solid water. Then 2 cm of solid water was placed on top of the flasks to provide a buildup region. The flasks were exposed to a 6-MV X-ray beam at a gantry angle of 0^{o} and field size of 20 × 20 cm.

study. The 3-Gy dose was chosen as an approximate clinical fractional dose consistent with that used in an earlier study (Karshafian et al. 2010), while the 6-Gy dose was selected as the highest dose deliverable in a reasonable time frame within the limitations of the 6 mGy/s dose rate. Radiation field uniformity and coverage were validated in the x- and y-planes for all radiation setups using Gafchromic film (data not shown).

Post-treatment

After treatments, the flasks were transported back to the laboratory where they were returned to the incubator for a few minutes while the laminar flow hood was prepared. Once flasks were examined under the microscope to confirm cells were still detached, flask contents were transferred to a 50-mL tube and centrifuged (200*g* for 5 min) to remove any residual treatment compounds. Cells were then resuspended in a T25 flask containing 10 mL of complete medium and returned to the incubator. After 24 h, the tissue culture medium was replenished, and 48 h later cell viability was measured using the MTS assay.

Cell viability measurements

At ~72 h after treatment, the medium was removed from each flask, and replaced with 1 mL of supplement-free (*i.e.,* Incomplete) tissue culture medium and 200 μL of MTS at a ratio of 5:1 per the manufacturer's instructions (Promega Corp. 2012). Four technical replicates of 100 μL of incomplete medium plus 20 μL of MTS were plated in a 96-well plate to act as medium blanks. Flasks and plates were then returned to the incubator for the development times stated earlier. Four technical replicates of 120 μL from each flask were then transferred to the 96-well plate, and the plate was read at 490 nm using a CLARIOstar Plus Plate reader (BMG Labtech, Mornington, Australia). The average of the four technical replicates was calculated for each condition, and the average of the four blank wells subtracted to give the final raw absorbance reading for each condition. Values for the three control flasks were averaged within each experiment, and the standard deviation (SD) calculated.

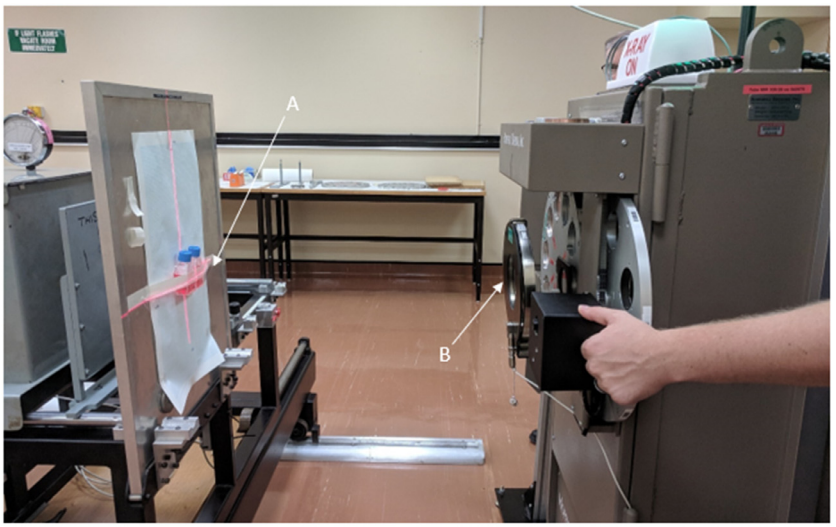

Fig. 3. Image of experimental setup for kilovolt X-ray exposures. Treatment flasks taped vertically to the baseplate (A) of the Model X80 X-Ray Beam irradiator (B). The source-to-surface distance was set at 100 cm to the front of the baseplate.

Normalized survival was then calculated by dividing the raw absorbance values for each treatment condition by the averaged raw absorbance control value for each experiment.

Statistical analysis

Overall normalized survival was averaged across the three repeats of the same experiment, and the SD was calculated using Excel. The key assumptions of the analysis of variance (ANOVA) test were initially validated in SPSS version 27 software (IBM, Armonk, NY, USA), using the Shapiro−Wilk (SW) test to confirm the normality of distributions; Levine's test to confirm the homogeneity of error variance (LHEV); and outliers identified visually on the box-and-whisker plot as flagged by the software (Gignac 2019; Laerd Statistics 2018). Statistical significance between treatment groups was then determined via a three-way ANOVA using a 2 × 3 × 2 design to report on the two levels of USMB (*i.e.,* presence or absence); three radiation dose levels of 0, 3 and 6 Gy; and two radiation energies of kilovolt and MV X-rays. *Post hoc* analysis included pairwise *t*-tests, with p values <0.05 reported as statistically significant (Fay and Gerow 2018). Where the LHEV revealed unequal variances, data were re-analyzed using a one-way Welch's ANOVA with Games−Howell *post hoc* testing after re-expressing the 2 × 3 × 2 design as a one-way subprogram (Fay and Gerow 2018; Gignac 2019).

RESULTS

NCI-H727 cells

Three-way ANOVA revealed statistically significant decreases in irradiated NCI-H727 cell survival across all RT dose levels and energies through the addition of USMB (Fig. 4). USMB alone in the absence of radiation resulted in significant cell death, producing a large, extremely significant overall difference in normalized survival compared with untreated controls ($\eta_p^2 = 0.776$, $p < 0.0001$).

No overall difference in normalized cell survival was seen between cells treated with kV X-rays and those treated with MV X-rays ($\eta_p^2 = 0.025$, $p = 0.420$), with comparisons between equivalent cohorts treated using the same radiation dose levels and USMB conditions revealing no significant difference in survival between the two radiation energies.

Radiation dose had the largest overall effect ($\eta_p^2 = 0.796$, $p < 0.0001$), with normalized survival decreasing as radiation dose increased. However, dose−response analysis revealed only one significant decrease in normalized survival (NS) in response to increases in radiation dose, and this was for cells treated with 3 Gy compared with 6 Gy of kV radiation in the absence of USMB (NS = 0.62 for 3 Gy kV alone vs. NS = 0.47 for 6 Gy kV alone, $p = 0.031$). Almost no dose response was detected when radiation dose was increased from 3 to 6 Gy of MV radiation in the presence of USMB (NS = 0.36 for USMB + 3 Gy MV vs. NS = 0.35 for USMB + 6 Gy MV, $p = 0.868$).

FTC-238 cells

Decreases in normalized cell survival were observed through the addition of USMB; however, these was not statistically significant for FTC-238 cells as determined with Welch's ANOVA (Fig. 5). Unlike the NCI-H727 cells, treatment with USMB alone had little effect on FTC-238 cell survival compared with untreated controls, with only a small decrease in survival observed for the kV cohort (NS = 0.93 for kV, NS = 1.0 for MV).

A slight increase in overall cell kill was observed for cells treated with kV compared with MV radiation; however, pairwise comparisons between equivalent treatment conditions were statistically significant only for the USMB + 6 Gy cohorts (NS = 0.46 for USMB + 6 Gy kV vs. NS = 0.60 for USMB + 6 Gy MV, $p = 0.038$).

For MV radiation, consistent decreases in survival with increases in dose were seen for both MV-alone and USMB + MV cohorts; however, these were not significant at any dose level. Normalized survival decreased by 0.17 when radiation dose was increased from 0 to 3 Gy in both the absence and presence of USMB, respectively (*i.e.,* 0−3Gy MV-alone vs. USMB + 0−3 Gy MV). This trend continued as dose was increased from 3 to 6 Gy, with further decreases in survival of 0.21 and 0.23. For kV radiation, however, much larger decreases in survival were observed at lower doses, with normalized survival decreasing by 0.30 and 0.33 from 0 to 3 Gy for kV alone compared with USMB + kV. However, further dose increases from 3−6 Gy yielded a more diminished response in the USMB + kV cohorts, where a decrease of 0.14 was seen for USMB +3 Gy kV and USMB + 6 Gy kV compared with 0.21 between 3 Gy kV alone and 6 Gy kV alone.

Human umbilical vein endothelial cells

Much like the FTC-238 cells, decreases in normalized cell survival were observed through the addition of USMB; however, these was not statistically significant for HUVEC as determined with Welch's ANOVA (Fig. 6). Non-significant variations in cell survival were observed when HUVEC were treated with USMB alone. For the MV cohort, a decrease in cell survival compared with untreated controls was seen, while an increase was noted for the kV group (0.92 for MV compared with 1.06 for kV).

No statistically significant differences were observed in cells treated using kV versus MV radiation,

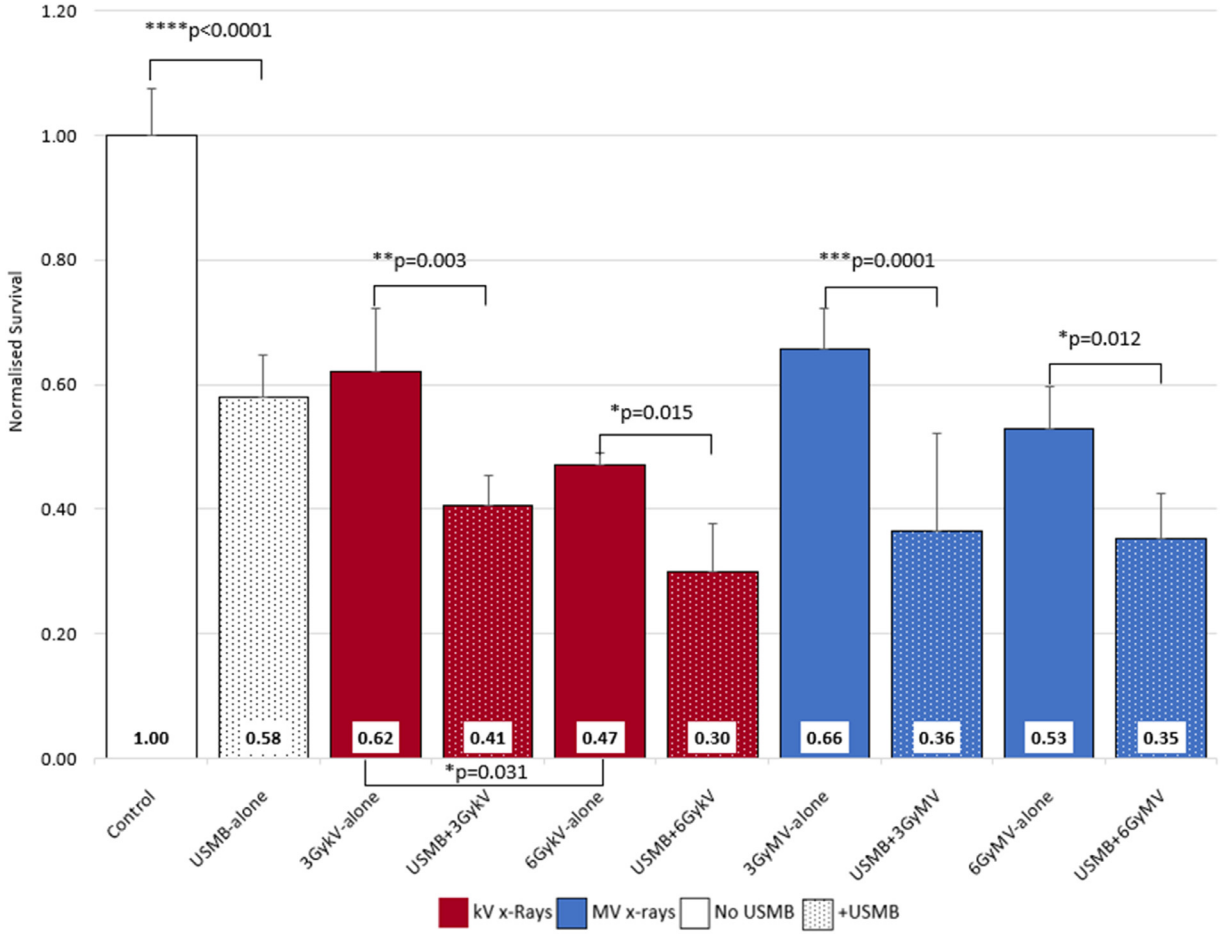

Fig. 4. Effect of USMB + RT on the viability of NCI-H727 cells. Cells were treated with 1.6% MB, ~90 s of US and either 0, 3 or 6 Gy of kV (*red*) and MV (*blue*) X-rays. Results are expressed as the mean + standard deviation for three biological replicates. The value for the untreated controls was assigned as unity (1), and the values for the treated cells were expressed as a fraction of this number. Both kV and MV experiments were carried out concurrently for this cell line. Significance values were calculated using a three-way analysis of variance. kV = kilovolt; MV = megavolt; RT = radiation therapy; USMB = ultrasound-stimulated microbubbles.

with the largest mean difference between equivalent conditions observed in the USMB + 3 Gy cohorts (NS = 0.45 for USMB + 3 Gy kV vs. NS = 0.61 for USMB + 3 Gy MV, $p = 0.95$).

A statistically significant dose−response relationship was seen across all radiation doses for cells treated using kV radiation in the absence of USMB. Normalized survival decreased by 0.46 when radiation dose was increased from 0 to 3 Gy ($p < 0.0001$) and by 0.19 when increased from 3 to 6 Gy ($p = 0.037$). A similar trend was observed with the addition of USMB; however, this was statistically significant only for the 0- to 3-Gy dose level increase (NS decreased by 0.61, $p = 0.024$, for 0−3 Gy, compared with 0.11, $p = 0.167$, for 3−6 Gy). For cells treated with MV radiation, non-significant decreases in survival were consistent across the two dose levels, with the greatest difference observed when radiation dose was increased from 0 to 3 Gy MV in the absence of USMB (survival decreased by 0.35 between the 0- and 3-Gy MV-alone cohorts, and 0.22 between 3 and 6 Gy, compared with 0.27 between 0- and 3-Gy USMB + MV and 0.27 between 3- and 6-Gy USMB + MV).

DISCUSSION

This study was aimed at investigating the role of USMB in directly enhancing radiation-induced tumor cell killing *in vitro*, given the conflicting results previously reported elsewhere. As there was strong evidence to support the effect as being cell type dependent, a variety of cell types were used, with a focus on lung tumors given the potential benefit

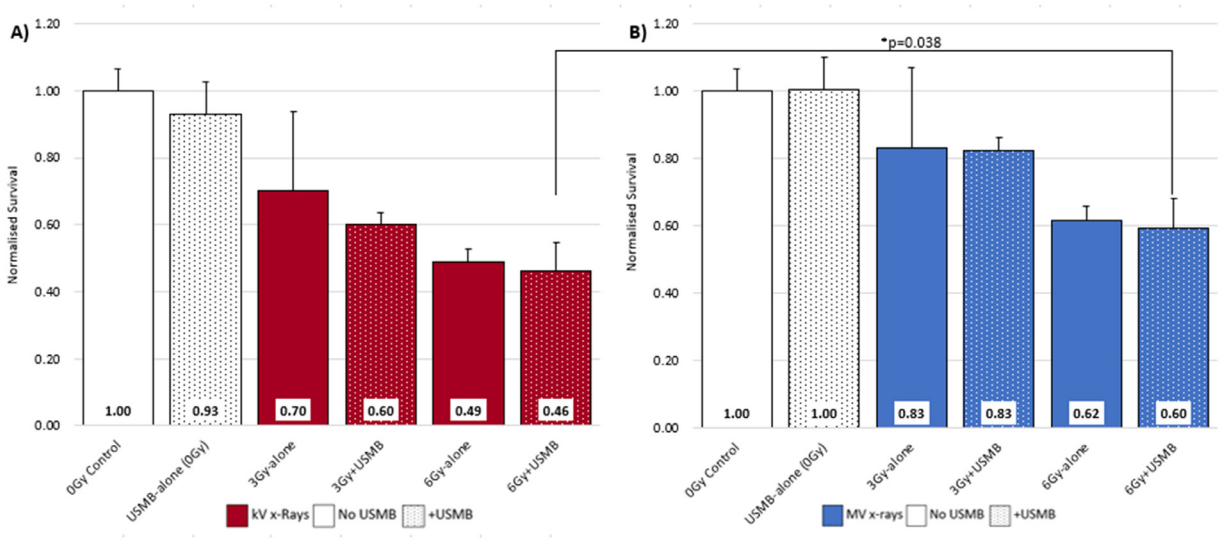

Fig. 5. Effect of USMB + RT on the viability of FTC-238 cells. Cells were treated with 1.6% MB, ~90 s of US and either 0, 3 or 6 Gy of (A) kV (*red*) and (B) MV(*blue*) X-rays. Results are expressed as the mean + standard deviation for three biological replicates. The value for the untreated controls was assigned as unity (1), and the values for the treated cells were expressed as a fraction of this number. Significance values were calculated using Welch's analysis of variance as the data did not demonstrate homogeneity of variances. kV = kilovolt; MV = megavolt; RT = radiation therapy; USMB = ultrasound-stimulated microbubbles.

radiosensitization may have in overcoming challenges of radiotherapy treatment delivery to the chest (Piperdi et al. 2021). Both kV and MV energies were also used to investigate radiation energy as another potential source of the reported variation, as no direct comparison between the two has been investigated to date, despite both being used in previous studies.

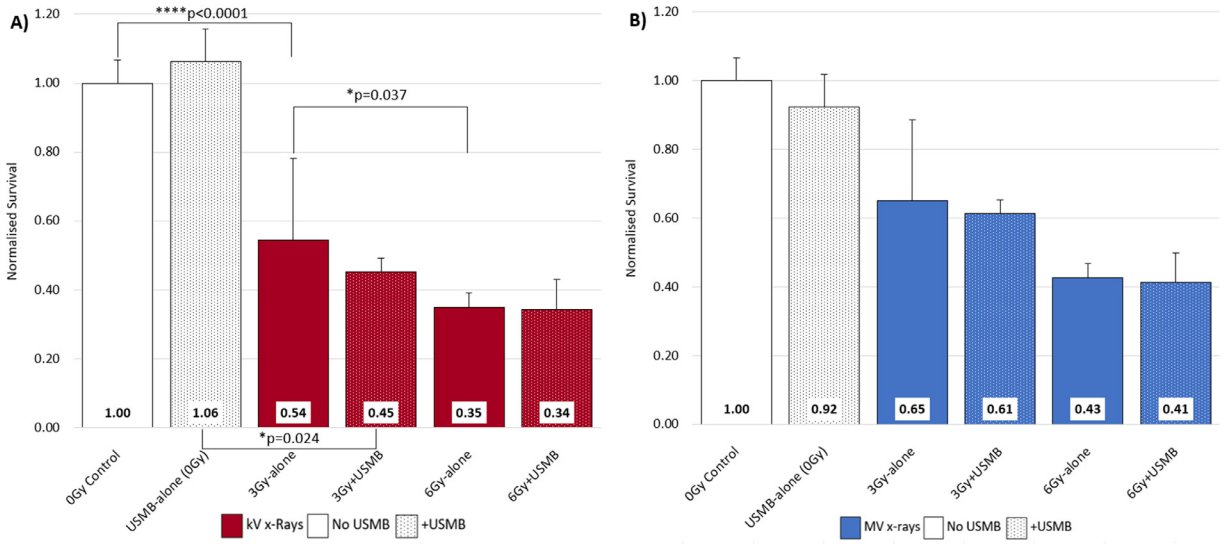

Fig. 6. Effect of USMB + RT on the viability of human umbilical vein endothelial cells. Cells were treated with 1.6% MB, ~90 s of US and either 0, 3 or 6 Gy of (A) kV and (B) MV x-rays. Results expressed as the mean + standard deviation for three biological replicates. The value for the untreated controls was assigned as unity (1), and the values for the treated cells were expressed as a fraction of this number. Significance values were calculated using a Welch's analysis of variance (ANOVA) as the data did not demonstrate homogeneity of variances. kV = kilovolt; MV = megavolt; RT = radiation therapy; USMB = ultrasound-stimulated microbubbles.

USMB directly enhance radiation-induced tumor cell killing in vitro *in a cell type- dependent manner*

Our results indicated that cells treated with combined USMB and radiation have decreased normalized survival compared with cells treated with radiation alone, with statistically significant effects observed for the NCI-H727 cells. USMB had a significant effect on the survival of irradiated NCI-H727 cells. This effect could be cell type dependent, which had been suggested earlier (El Kaffas and Czarnota 2015). These cell type-specific responses to USMB + RT have previously been linked to ASMase gene expression and ceramide signaling associated with apoptosis. This was determined by Nofiele et al. (2013) using ASMase deficient$^{-/-}$ astrocytes and ASMase$^{+/+}$ astrocytes treated with sphingosine-1-phosphate (S1P) to counteract the ceramide-mediated apoptosis pathway. ASMase$^{+/+}$ astrocytes were more sensitive to USMB + RT compared with ASMase$^{-/-}$ or S1P-ASMase$^{+/+}$ astrocytes where ASMase and ceramide production had been genetically or chemically inhibited. As NCI-H727 cells elicited a strong response to USMB + RT, changes in ASMase gene expression and ceramide levels produced in response to this treatment should be investigated to determine whether this could be used as an indicator of cell sensitivity to such treatments. In a study of pre-operative blood serum samples extracted from 61 patients diagnosed with NSCLC, significantly increased levels of ASMase activity were detected compared with those in healthy controls (Kachler et al. 2017), which may explain why the NSCLC cell line investigated here exhibited such a strong response compared with the other two cell lines. Immunostaining cells for ASMase activity and/or ceramide production may be of benefit in future studies—both as a screening tool to identify candidate cells lines for further USMB + RT research and to better understand responses to USMB + RT treatment.

Given the increased risks associated with delivering radiotherapy to centrally lying lung tumors (Wu et al. 2014; Haseltine et al. 2016), methods of localized radiotherapy sensitization as offered by USMB are of particular interest. The identification of specific cell types demonstrating radiosensitization effects through the addition of USMB provides exciting avenues for further research with direct clinical relevance. Although the logistics of microbubble delivery and ultrasound administration to the chest may require further optimization, solutions may be found in other areas of research, such as nanoparticle radiosensitization research, in which direct tumoral injection and inhalation administration methods have been investigated (Boateng and Ngwa 2019). Given microbubbles have long been used as a contrast agent to improve cardiac ultrasound imaging, microbubble stimulation of centrally lying lung tumors proximal to the mediastinum is not unfeasible and could be investigated further.

HUVEC, however, have also been reported to have ~20-fold higher levels of ASMase compared with other cells (Marathe et al. 1998), and so should have also exhibited decreased viability when treated with USMB + RT in this study if ASMase gene expression is the primary mechanism involved. Further investigations of other factors that may be responsible for the dramatic effect USMB have on the viability of irradiated NCI-727 cells are underway. These factors include the use of T12.5 flasks, as the acoustic field applied to the NCI-H727 cells may have differed from that applied to the HUVEC and FTC-238 cells treated in T25 flasks, potentially resulting in differences in the level of sonoporation effects on these cells. Kinoshita and Hynynen (2007) reported that cell viability was substantially decreased in the presence of standing waves, and the interaction of the US field with the T12.5 flask may have created such a phenomenon, which was absent in the T25 flasks. It is interesting to note that this study also reported differences in cell viability when cells were exposed to USMB in a suspended state compared with an adherent state. Lammertink et al. (2016) also exposed the cells in an adherent state, further introducing yet another point of difference from all other research using USMB + RT in which cells were treated in suspension. This may also explain why their results were so different and is another factor under investigation.

Although slight dose enhancement was noted for HUVEC treated with USMB + RT compared with those treated with RT alone, the difference was not significant and less than that seen in previous studies (Al-Mahrouki et al. 2012, 2015; Nofiele et al. 2013). This difference could be related to the experimental setup, in which different cell numbers and culture vessels, MB concentrations, US applications, and x-ray fields were used. The 1.6% (v/v) MB concentration used in the current study was less than the 3.3% (v/v) used in those studies on HUVEC. MB concentrations were reported to be optimal at 1.6% (v/v) in enhancing the effect of RT on acute myeloid leukemia cells (Karshafian et al. 2009); however, Lammertink et al. (2016) observed no significant difference in the survival of FaDU cells when MB at 7% (v/v) were added to cells exposed to RT. Unlike HUVEC, the effect of MB on the cytotoxic effect of RT has not been examined for either FTC-238 and NCI-H727 cells, and as such, 1.6% v/v was chosen as the MB concentration to use in these experiments. As the effects elicited with 1.6% (v/v) MB on the cytotoxic effect of RT on HUVEC reported here were less than those seen in earlier studies (Al-Mahrouki et al. 2012, 2015; Nofiele et al. 2013), repeat experiments using 3.3% (v/v) are now warranted. Similarly, further quantification of the exact

ultrasound pressures applied to the microbubbles may be of benefit, given the differences in the ultrasound equipment used in this study compared with previous studies (*i.e.,* the use of a diagnostic US probe here compared with those used specifically for US research).

Radiation energy is not a likely influence on results

The FTC-238 cells are derived from a metastatic tumor deposit of a follicular thyroid carcinoma. The addition of MB at 1.6% (v/v) did not have a significant effect on the viability of these secondary tumor cells when exposed to either kV or MV radiation. Of interest was that at the same dose (3 or 6 Gy), kV radiation was more cytotoxic than MV radiation, with a statistically significant result observed between USMB + 6 Gy kV and USMB + 6 Gy MV. This difference between the cytotoxic effect elicited by kV and MV radiation was seen to a much lesser extent in the HUVEC, where a similar trend was observed; however, no statistically significant differences were seen between cohorts treated using the same radiation dose levels and USMB conditions using either kV or MV radiation. For the NCI-H727 cells, three-way ANOVA revealed no overall difference in normalized cell survival for cells treated using kV compared with MV X-rays, suggesting that for this cell line in particular, radiation energy has little influence on results.

It is unlikely that such responses to differences in radiation energy are cell type dependent and are more likely due to the differences in raw absorbance readings recorded for the control flasks, which varied by ~26% between the two X-ray treatment types for the FTC-238 cell line. This could have arisen from differences in travel times to the various treatment facilities that resulted in these cells being out of the incubator for different lengths of time, or the difference in medium-to-cell ratio between the T12.5 and T25 flasks during the ~90-min treatment time. Subsequent research is required to investigate the impacts of these differences further.

In the study conducted by Lammertink et al. (2016), FaDU cells were exposed to MV X-rays, and the survival curves for cells treated with USMB + RT and those treated with RT were similar. This differs from other studies in which cells exposed to kV X-rays were treated with USMB and there was a reduction in cell survival rates (Karshafian et al. 2009, 2010; Deng et al. 2018). In our study, flasks of FTC-238 cells and HUVEC were exposed to kV and MV X-rays at different times, and it is unknown if a similar result would be obtained if the flasks were irradiated by both X-ray energies concurrently, as done for the NCI-H727 cells. We observed that in the NCI-727 cells, there was minimal difference in survival at similar dose levels for kV and MV X-rays, compared with the differences seen when the different cohorts were treated separately as for FTC-238 cells and HUVEC.

Responses to USMB alone may be a predictor of dose enhancement

The most likely explanation for the NCI-H727 results seen here is that these cells are inherently more sensitive to the effects of USMB, which is supported by the very highly significant difference ($p < 0.001$) in normalized survival between the control and USMB-only cohorts. Previous sonoporation studies have also determined different responses across cell lines of similar origin treated with USMB alone (Bjånes et al. 2020). Where the HUVEC and FTC-238 cells may benefit from increases in MB concentration, further experiments at lower concentrations for the NCI-H727 cells may be required to establishing toxicity profiles for US, MB and USMB alone in the absence of RT.

CONCLUSIONS

Although USMB did enhance radiation-induced cell killing *in vitro* in the cell lines examined, the difference was statistically significant only for NCI-H727 non-small cell lung carcinoma cells. This suggests that enhancement is most likely cell type dependent, which is consistent with previous findings in the literature. However, there may also be other factors influencing these results, such as variations in applied acoustic fields, differences in the cytotoxicity profiles for USMB alone and cell culture state (*i.e.,* suspension vs. adherent). Given the overall trends observed here, this study illustrates that this type of research is feasible using clinical hardware and that further opportunities exist to understand the specific mechanisms involved in the direct radiosensitization of tumor cells using USMB.

DECLARATION OF COMPETING INTEREST

The authors declare no conflict of interest.

Acknowledgments—The authors thank the Australian Radiation Protection and Nuclear Safety Agency and the staff at GenesisCare Epping Radiation Oncology Centre for their support and use of their equipment. They also acknowledge the Australian Government's Department of Education and Training for providing financial support via the Joint Research Engagement Engineering Cadetship.

REFERENCES

Al-Mahrouki AA, Karshafian R, Giles A, Czarnota GJ. Bioeffects of ultrasound-stimulated microbubbles on endothelial cells: Gene expression changes associated with radiation enhancement in vitro. Ultrasound Med Biol 2012;38:1958–1969.

Al-Mahrouki AA, Iradji S, Tran WT, Czarnota GJ. Cellular characterization of ultrasound-stimulated microbubble radiation enhancement in a prostate cancer xenograft model. Dis Model Mech 2014;7:363.

Al-Mahrouki AA, Wong E, Czarnota GJ. Ultrasound-stimulated microbubble enhancement of radiation treatments: Endothelial cell function and mechanism. Oncoscience 2015;2:944–957.

Bjånes T, Kotopoulis S, Murvold ET, Kamčeva T, Gjertsen BT, Gilja OH, Schjøtt J, Riedel B, McCormack E. Ultrasound- and microbubble-assisted gemcitabine delivery to pancreatic cancer cells. Pharmaceutics 2020;12:141.

Boateng F, Ngwa W. Delivery of nanoparticle-based radiosensitizers for radiotherapy applications. Int J Mol Sci 2019;21:273.

Buch K, Peters T, Nawroth T, Sänger M, Schmidberger H, Langguth P. Determination of cell survival after irradiation via clonogenic assay versus multiple MTT assay—A comparative study. Radiat Oncol 2012;7:1–6.

Czarnota GJ, Karshafian R, Burns PN, Wong S, Al Mahrouki A, Lee JW, Caissie A, Tran W, Kim C, Furukawa M. Tumor radiation response enhancement by acoustical stimulation of the vasculature. Proc Natl Acad Sci USA 2012;109:E2033–E2041.

Daecher A, Stanczak M, Liu JB, Zhang J, Du S, Forsberg F, Leeper DB, Eisenbrey JR. Localized microbubble cavitation-based antivascular therapy for improving HCC treatment response to radiotherapy. Cancer Lett 2017;411:100–105.

Deng H, Cai Y, Feng Q, Wang X, Tian W, Qiu S, Wang Y, Li Z, Wu J. Ultrasound-stimulated microbubbles enhance radiosensitization of nasopharyngeal carcinoma. Cell Physiol Biochem 2018;48:1530–1542.

Dimcevski G, Kotopoulis S, Bjånes T, Hoem D, Schjøtt J, Gjertsen BT, Biermann M, Molven A, Sorbye H, McCormack E. A human clinical trial using ultrasound and microbubbles to enhance gemcitabine treatment of inoperable pancreatic cancer. J Control Release 2016;243:172–181.

Dos Santos M, Paget V, Ben Kacem M, Trompier F, Benadjaoud MA, François A, Guipaud O, Benderitter M, Milliat F. Importance of dosimetry protocol for cell irradiation on a low X-rays facility and consequences for the biological response. Int J Radiat Biol 2018;94:597–606.

Ebben HP, Nederhoed JH, Lely RJ, Wisselink W, Yeung K. Microbubbles and ultrasound-accelerated thrombolysis (MUST) for peripheral arterial occlusions: Protocol for a phase II single-arm trial. BMJ Open 2017;7 e014365.

Eisenbrey JR, Shraim R, Liu JB, Li J, Stanczak M, Oeffinger B, Leeper DB, Keith SW, Jablonowski LJ, Forsberg F. Sensitization of hypoxic tumors to radiation therapy using ultrasound-sensitive oxygen microbubbles. Int J Radiat Oncol Biol Phys 2018;101:88–96.

El Kaffas A, Czarnota GJ. Biomechanical effects of microbubbles: From radiosensitization to cell death. Future Oncol 2015;11:1093–1108.

Fan Z, Kumon RE, Deng CX. Mechanisms of microbubble-facilitated sonoporation for drug and gene delivery. Ther Deliv 2014;5:467–486.

Fay DS, Gerow K. WormBook: The online review of *C. elegans* biology [Internet]. Available at: https://www.ncbi.nlm.nih.gov/books/NBK153593/. Accessed March 20, 2020.

Gignac GE. How2statsbook. Available at: https://sites.google.com/site/how2statsbook1/Table%20of%20Contents%20-%202019.pdf?attredirects=0&d=1. Accessed July 8, 2020.

Goretzki P, Frilling A, Simon D, Roeher HD. Growth regulation of normal thyroids and thyroid tumors in man. In: Hormone-related malignant tumors. Berlin/Heidelberg: Springer; 1990. p. 48–63.

Haseltine JM, Rimner A, Gelblum DY, Modh A, Rosenzweig KE, Jackson A, Yorke ED, Wu AJ. Fatal complications after stereotactic body radiation therapy for central lung tumors abutting the proximal bronchial tree. Pract Radiat Oncol 2016;6:e27–e33.

Kachler K, Bailer M, Heim L, Schumacher F, Reichel M, Holzinger CD, Trump S, Mittler S, Monti J, Trufa DI, Rieker RJ, Hartmann A, Sirbu H, Kleuser B, Kornhuber J, Finotto S. Enhanced acid sphingomyelinase activity drives immune evasion and tumor growth in non–small cell lung carcinoma. Cancer Res 2017;77:5963–5976.

Karshafian R, Giles A, Burns PN, Czarnota GJ. Ultrasound-activated microbubbles as novel enhancers of radiotherapy in leukemia cells in vitro. Proc IEEE Int Ultrason Symp 2009;1792–1794.

Karshafian R, Tchouala JIN, Al-Mahrouki A, Giles A, Czarnota GJ. Enhancement of radiation therapy by ultrasonically-stimulated microbubbles in vitro: Effects of treatment scheduling on cell viability and production of ceramide. Proc IEEE Int Ultrason Symp 2010;2115–2118.

Kaul S. Myocardial contrast echocardiography: A 25-year retrospective. Circulation 2008;118:291–308.

Kinoshita M, Hynynen K. Key factors that affect sonoporation efficiency in in vitro settings: The importance of standing wave in sonoporation. Biochem Biophys Res Commun 2007;359:860–865.

Laerd Statistics. Testing for Normality using SPSS Statistics when you have only one independent variable. Available at: https://statistics.laerd.com/spss-tutorials/testing-for-normality-using-spss-statistics.php. Accessed October 9, 2020.

Lai P, Tarapacki C, Tran WT, El Kaffas A, Lee J, Hupple C, Iradji S, Giles A, Al-Mahrouki A, Czarnota GJ. Breast tumor response to ultrasound mediated excitation of microbubbles and radiation therapy in vivo. Oncoscience 2016;3:98–108.

Lammertink BHA, Bos C, van der Wurff-Jacobs KM, Storm G, Moonen CT, Deckers R. Increase of intracellular cisplatin levels and radiosensitization by ultrasound in combination with microbubbles. J Control Release 2016;238:157–165.

DEFINITY®. Package insert. Lantheus Medical Imaging, Inc.; 2013.

Lentacker I, De Cock I, Deckers R, De Smedt SC, Moonen CTW. Understanding ultrasound induced sonoporation: Definitions and underlying mechanisms. Adv Drug Deliv Rev 2014;72:49–64.

Liu Y, Miyoshi H, Nakamura M. Encapsulated ultrasound microbubbles: Therapeutic application in drug/gene delivery. J Control Release 2006;114:89–99.

Marathe S, Schissel SL, Yellin MJ, Beatini N, Mintzer R, Williams KJ, Tabas I. Human vascular endothelial cells are a rich and regulatable source of secretory sphingomyelinase: Implications for early atherogenesis and ceramide-mediated cell signaling. J Biol Chem 1998;273:4081–4088.

Nofiele JIT, Karshafian R, Furukawa M, Al Mahrouki A, Giles A, Wong S, Czarnota GJ. Ultrasound-activated microbubble cancer therapy: Ceramide production leading to enhanced radiation effect in vitro. Technol Cancer Res Treat 2013;12:53–60.

Osei E, Al-Asady A. A review of ultrasound-mediated microbubbles technology for cancer therapy: A vehicle for chemotherapeutic drug delivery. J Radiother Pract 2020;19:291–298.

Piperdi H, Portal D, Neibart SS, Yue NJ, Jabbour SK, Reyhan M. Adaptive radiation therapy in the treatment of lung cancer: An overview of the current state of the field. Front Oncol 2021;11 770382.

Promega Corp. CellTiter 96® AQueous One Solution Cell Proliferation Assay. Available at: https://www.promega.com.au/products/cell-health-assays/cell-viability-and-cytotoxicity-assays/celltiter-96-aqueous-one-solution-cell-proliferation-assay-_mts_/?catNum=G3582. Accessed August 30, 2017.

Smith DJ, Jaggi M, Zhang W, Galich A, Du C, Sterrett SP, Smith LM, Balaji K. Metallothioneins and resistance to cisplatin and radiation in prostate cancer. Urology 2006;67:1341–1347.

Takahashi T, Nau MM, Chiba I, Birrer MJ, Rosenberg RK, Vinocour M, Levitt M, Pass H, Gazdar AF, Minna JD. p53: A frequent target for genetic abnormalities in lung cancer. Science 1989;246:491–494.

Wang Y, Li Y, Yan K, Shen L, Yang W, Gong J, Ding K. Clinical study of ultrasound and microbubbles for enhancing chemotherapeutic sensitivity of malignant tumors in digestive system. Chin J Cancer Res 2018;30:553–563.

World Health Organization. Cancer. Available at: https://www.who.int/news-room/fact-sheets/detail/cancer. Accessed February 26, 2022.

Wu AJ, Williams E, Modh A, Foster A, Yorke E, Rimner A, Jackson A. Dosimetric predictors of esophageal toxicity after stereotactic body radiotherapy for central lung tumors. Radiother Oncol 2014;112:267–271.

Youkhana EQ, Feltis B, Blencowe A, Geso M. Titanium dioxide nanoparticles as radiosensitisers: An in vitro and phantom-based study. Int J Med Sci 2017;14:602.

Zhu Q, Dong G, Wang Z, Sun L, Gao S, Liu Z. Intra-clot microbubble-enhanced ultrasound accelerates catheter-directed thrombolysis for deep vein thrombosis: A clinical study. Ultrasound Med Biol 2019;45:2427–2433.